Figure S1. Jia et al.

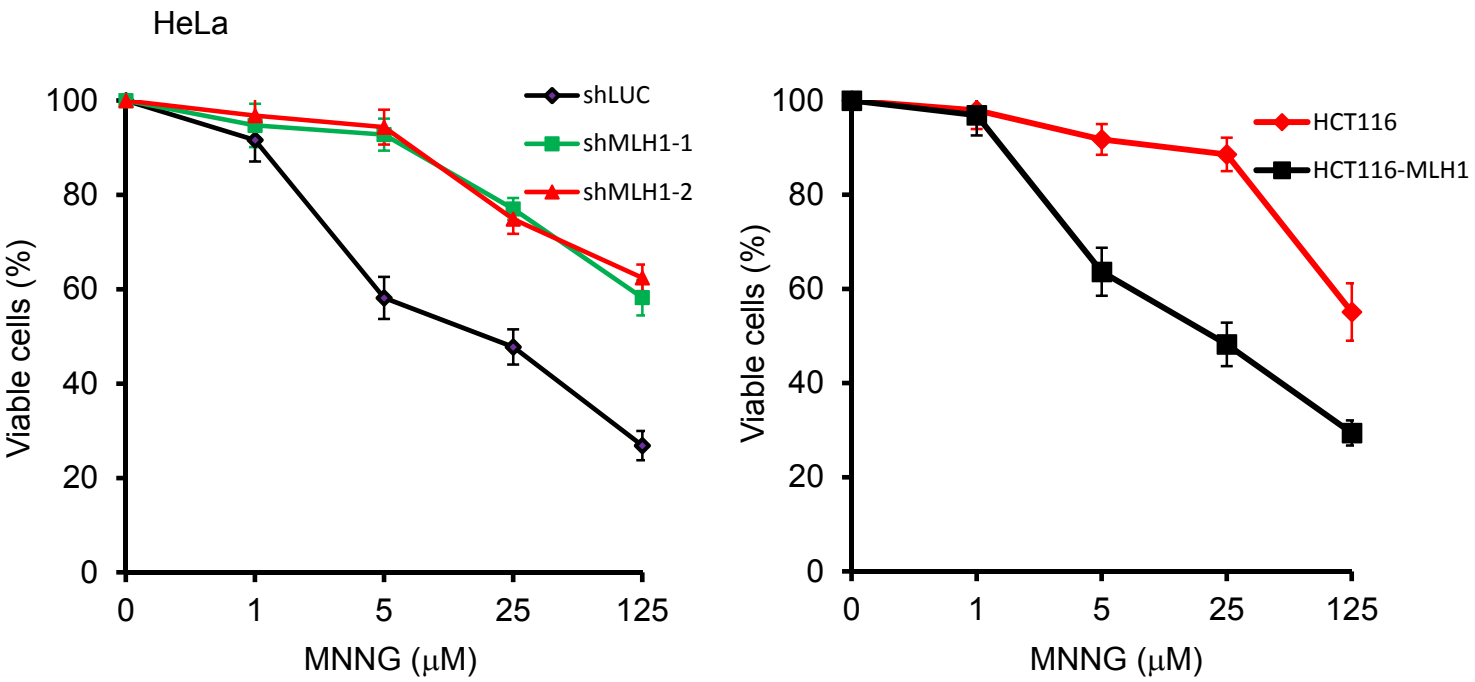

Figure S1. MLH1 deficient cells are resistant to the cytotoxic effect of MNNG. HeLa with MLH1 knockdown and MLH1-deficient HCT116 cells were treated with indicated concentrations of MNNG. Cell viability were measured by the MTT assay.

Figure S2. Jia et al.

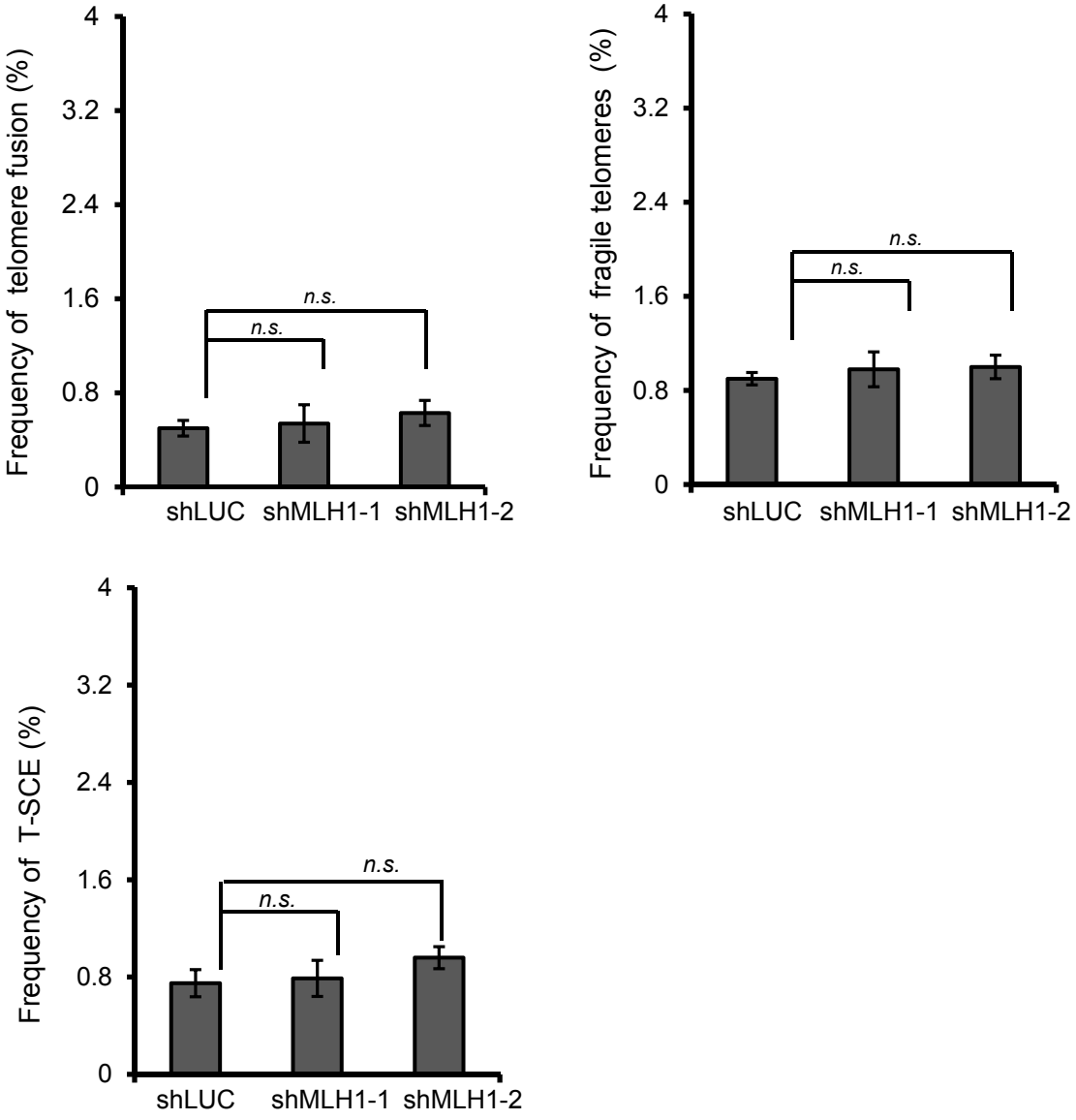

Figure S2. MLH1 deficiency does not induce telomere abnormalities. Metaphase chromosomes from HeLa MLH1 knockdown cells were hybridized by telomeric probe. In each experiment, >1,500 chromosomes from each sample were analyzed and each experiment was repeated with three independent replicates. Error bars: SEM.

Figure S3. Jia et al.

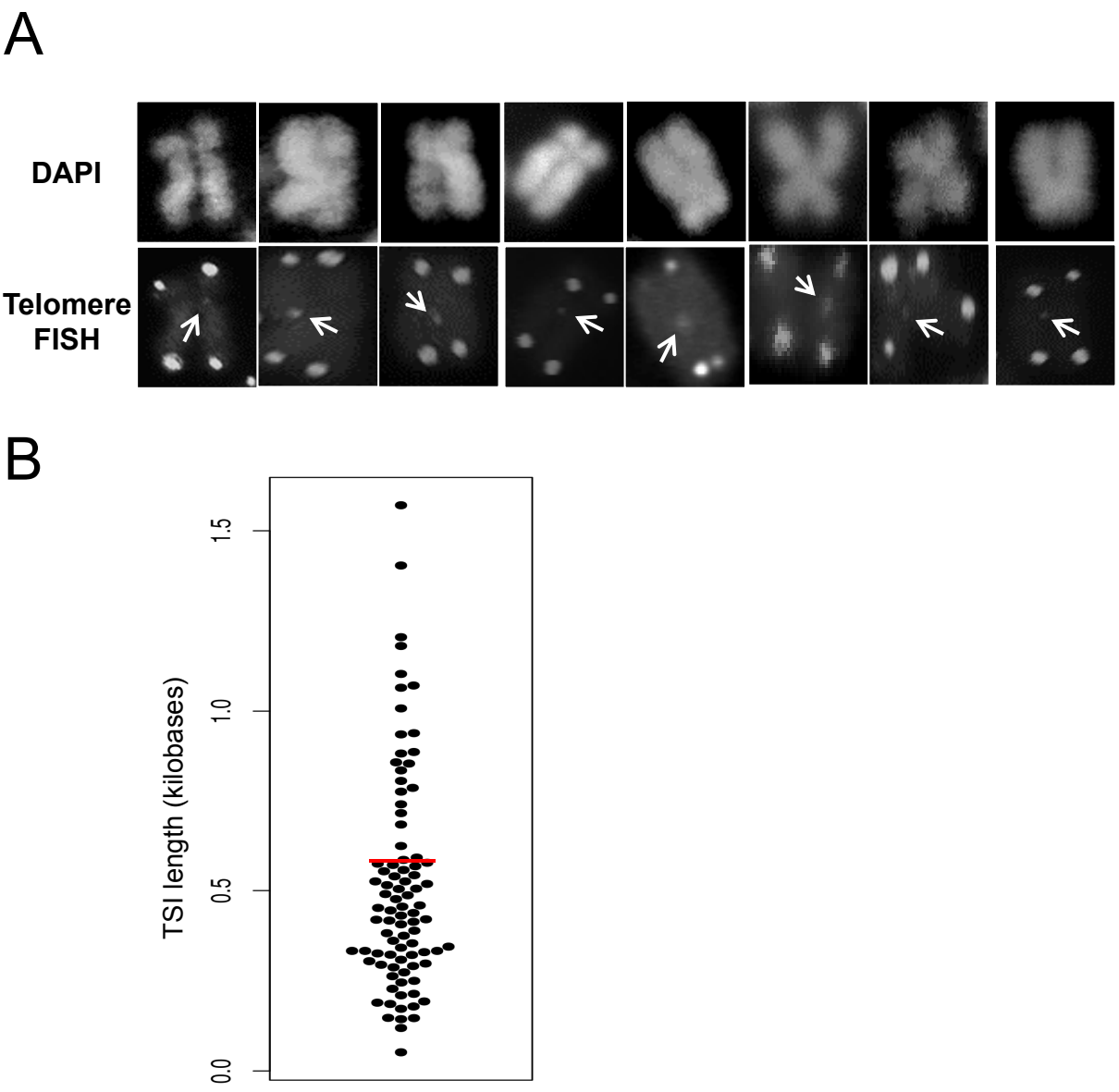

Figure S3. (A) The majority of TSI signals are weakly stained. Metaphase chromosomes from HCT116 cells were hybridized with telomeric probe. Eight randomly selected FISH images are shown. White arrows point to inserted telomeric sequences at intra-chromosomal loci. **(B) Calculated TSI length using Q-FISH.** Fluorescent intensity of individual TSIs (N_{TSI} = 89) were measured from HCT116 metaphase chromosomes. Red bar indicates the mean TSI length (578 bp).

Figure S4. Jia et al.

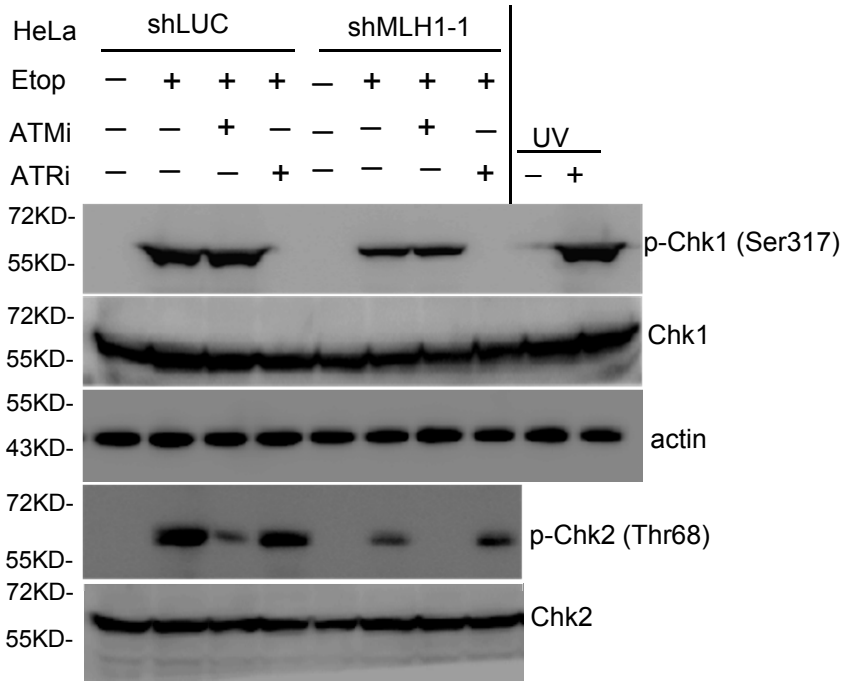

Figure S4. ATMi or ATRi abolishes ATM or ATR activation as measured by Chk1 or Chk2 phosphorylation. Immunoblot analysis of Chk1 and Chk2 phosphorylation in HeLa-shLUC and HeLa-shMLH1 cells. Cells were treated with ATM inhibitor (ATMi, 10 μM) or ATR inhibitor (ATRi, 10 μM) along with etoposide (3 μM). p-Chk1 (Ser317), Chk1, p-Chk2 (Thr68), Chk2 were detected by immunoblot. Untreated (UV-) and UV treated (UV+) plain HeLa cells were used as negative and positive controls for Chk1 phosphorylation.

Figure S5. Jia et al.

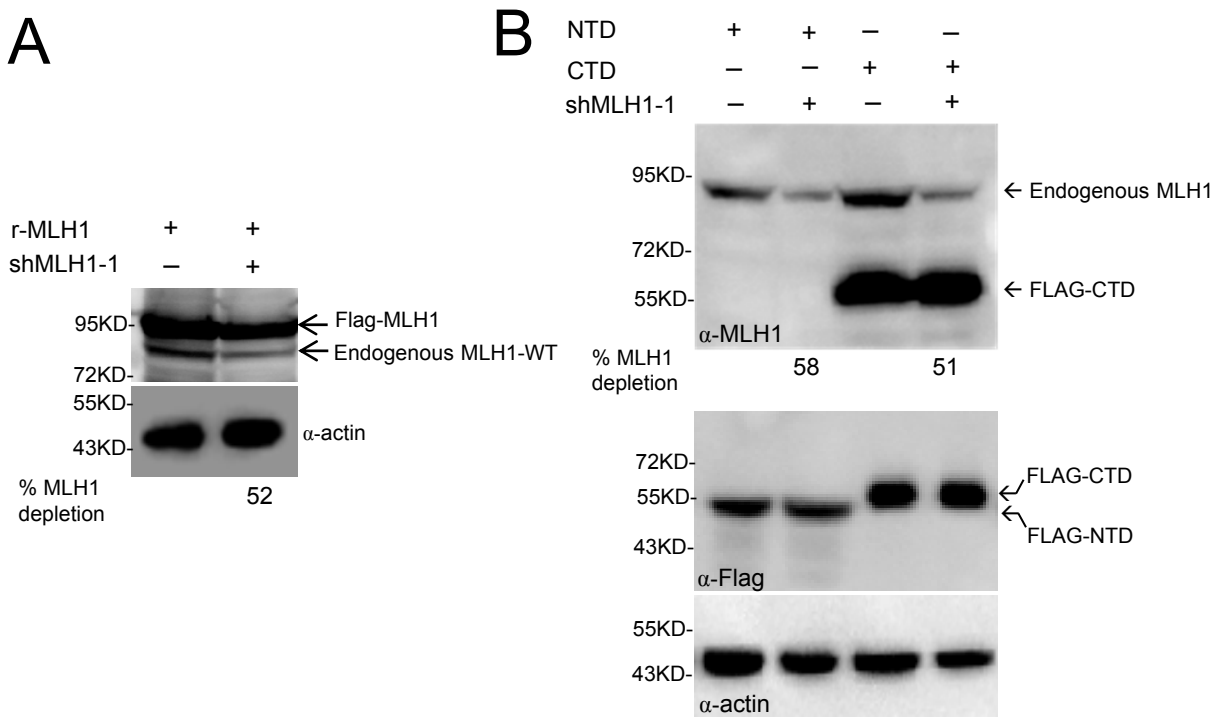

Figure S5. Immunoblot of endogenous MLH1 knockdown in cells expressing FLAG-MLH1 and MLH1 mutants. (A) Detection of knockdown of endogenous MLH1 in HeLa cells concurrently expressing shMLH1 and RNAi-resistant full-length FLAG-MLH1 (r-MLH1) with the MLH1 antibody. **(B)** Detection of knockdown of endogenous MLH1 in HeLa cells concurrently expressing shMLH1 and RNAi-resistant FLAG-NTD (2-389aa) or FLAG-CTD (390aa-756aa). Top panel: Immunoblot with anti-MLH1 antibody. Since the MLH1 antibody was produced by immunizing animals with truncated MLH1 protein (aa 381-483), it can only recognize CTD but not NTD. Middle panel: The expression of NTD and CTD was detected with the anti-FLAG antibody.

Figure S6. Jia et al.

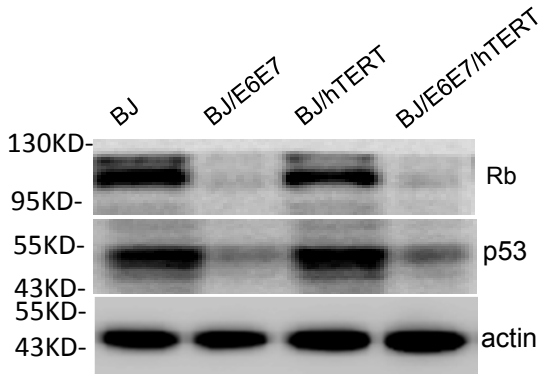

Figure S6. Expression of p53 and retinoblastoma (Rb) is repressed by E6 and E7. Immunoblot of p53 and Rb expression in BJ, BJ/hTERT, and corresponding cells expressing HPV E6 and E7 proteins.

Figure S7. Jia et al.

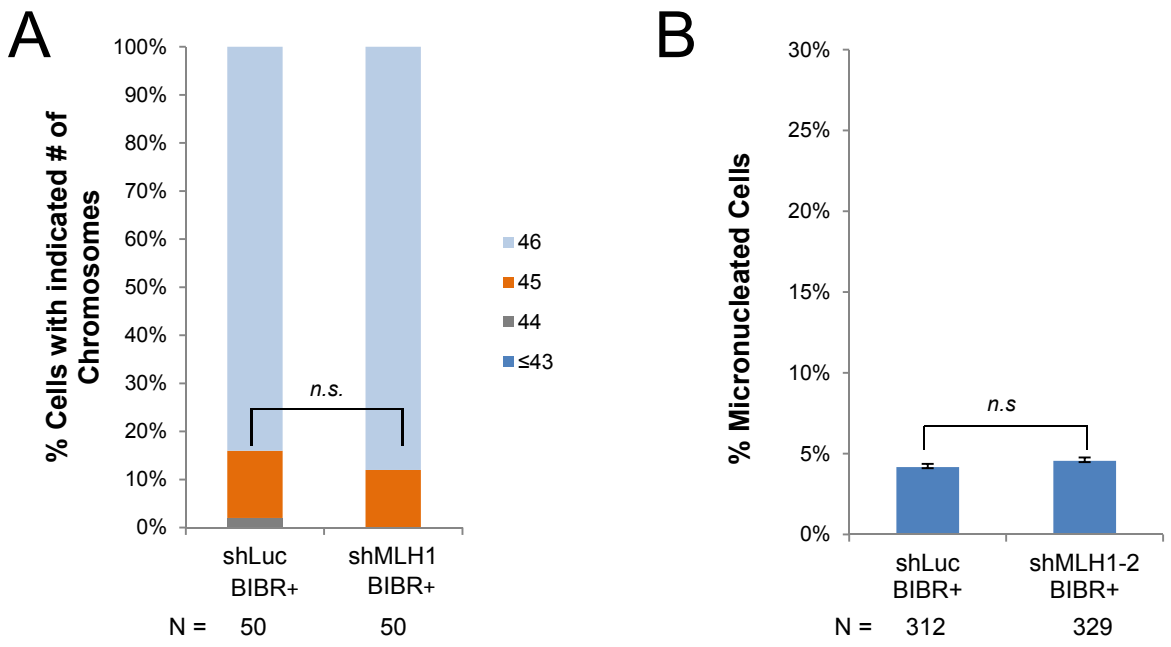

Figure S7. Chromosome loss and micronuclei formation are not induced by MLH1 deficiency in telomerase-negative cells. BJ/hTERT cells were treated with telomerase inhibitor BIBR and then analyzed for chromosome loss and MN formation. **(A)** Percentage of chromosome loss. N denotes the number of metaphase spreads analyzed in each sample. Chromosome loss was evaluated using a binomial Z-Statistic to compare the proportion of intact metaphase spreads (spreads with 46 chromosomes). **(B)** Percentage of micronucleated cells. N denotes the number of interphase cells analyzed in each sample.

Figure S8. Jia et al.

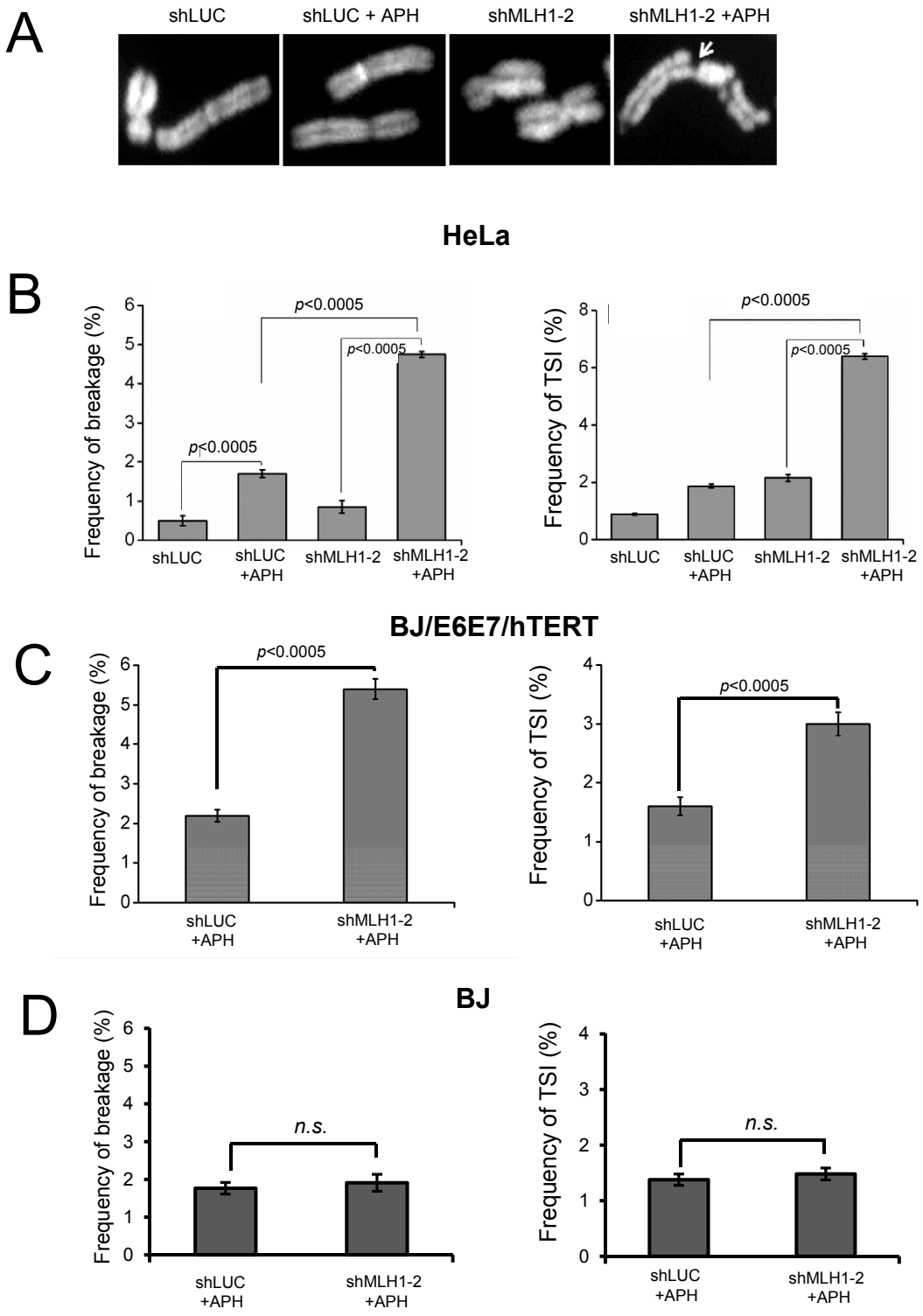

Figure S8. Chromosome breakage induced by MLH1 deficiency under replication stress. (A) Representative chromosomes in HeLa control and shMLH1 cells treated with or without APH (0.3 μM, 24 hrs). The white arrow indicates chromosomal breakage. **(B)** Frequency of chromosome breakage and TSI in control HeLa and MLH1 knockdown cells following APH treatment. **(C)** Frequency of chromosome breakages and %TSI in BJ/E6E7/hTERT control and shMLH1 cells following APH treatment. **(D)** Frequency of chromosome breakages and %TSI in BJ control and shMLH1 cells following APH treatment. In each experiment, >1,500 chromosomes from each sample were analyzed and each experiment was repeated with three independent replicates. Error bars: SEM.